Workspace Envelope Manipulation for Stewart Platform Simulators with Redundant Degrees of Freedom

Philipp Legran, Fabian Russ, Jobst Beckmann, Lutz Eckstein

Institute for Automotive Engineering (ika), RWTH Aachen University, philipp.legran@ika.rwth-aachen.de

Abstract - *This paper introduces a novel control scheme aimed at extending the workspace of hexapod-based dynamic driving simulators by exploiting redundant degrees of freedom. Dynamic driving simulators often face limitations in their ability to render motion due to workspace constraints imposed by the hexapod design. The proposed control algorithm optimizes the positioning in redundant degrees of freedom of the hexapod to maximize the workspace in non-redundant degrees of freedom. This is accomplished by determining a favorable position through an optimization algorithm, that minimizes a functional evaluated for the distance between the current actuator position and the actuator's limits.*

Keywords: *Dynamic Driving Simulator, Motion Cueing, Stewart Platform, Optimization, Workspace Envelope*

Introduction

Driving simulators are a crucial tool for studying the dynamics between vehicle occupants, vehicles, and their environment. Dynamic driving simulators provide the ability to render motion to reduce motion sickness in test subjects and increase the immersion of the simulation. Many simulators rely on Stewart platforms that can manipulate motion in three translational and three rotational degrees of freedom (DoF). Limited by the workspace envelope, the rendered accelerations and angular velocities can only be applied for brief amounts of time, need to be scaled down, or modified otherwise.

To overcome the workspace limitations imposed by the hexapod design, a secondary motion system can be superimposed to extend the motion limits for individual degrees of freedom. Common combinations include 7-DoF simulators (Zeeb, 2010), which consist of a linear rail and hexapod, and 8-DoF simulators (Baumann, et al., 2012), which allow for translation of the hexapod in two spatial dimensions. In addition, these simulators can be combined with a yaw table to extend the range of yaw motion (Fang, Wautier, and Kemeny, 2021).

The degrees of freedom of a hexapod in Cartesian space are strongly correlated. Moving the simulator in one degree of freedom can limit or extend the range of movement in another degree of freedom. When the hexapod is coupled with a superimposed motion system, the hexapod's workspace depends on the distribution of motion in the redundant degrees of freedom. Motion algorithms, such as classical washout algorithms for 7-DoFs, treat the hexapod and the superimposed motion system as independent entities and distribute motion based on physical performance (Ellensohn, et al., 2020).

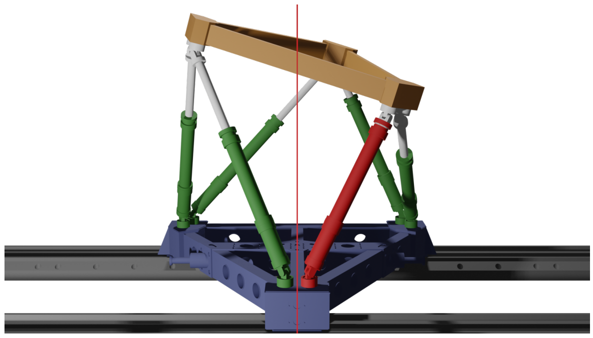

Figure 1: Invalid pose, one actuator below lower limit

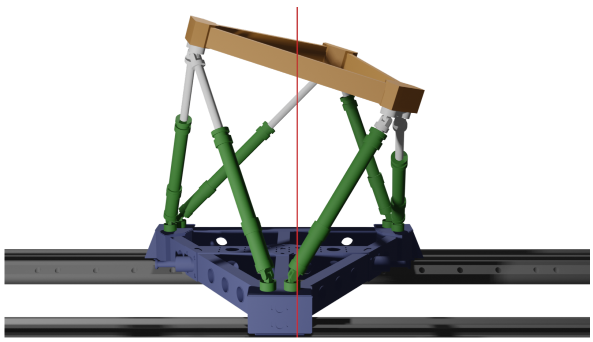

Figure 2: Valid pose, all actuators within limits

The interaction and effect on the remaining hexapod workspace is often neglected, leaving untapped potential.

A dynamic driving simulator with seven or more degrees of freedom allows for a hexapod motion in a redundant degree of freedom, that can be compensated by an opposite movement of the superimposed motion system. Thus, the hexapod working point can be manipulated without affecting the resulting global pose of the simulator. The control algorithm, that is investigated in this paper, exploits this behavior by shifting the operating point of the hexapod to extend the hexapod workspace in non-redundant degrees of freedom.

The following example demonstrates how a previously unattainable rotational pose can be achieved by translating in a redundant degree of freedom. Figure 1 shows a hexapod pose that is not valid because the right actuator is compressed beyond the limit. To decompress the right actuator, the rail sled can be moved to the left and the upper hexapod platform position, relative to the sled, can be translated to the right. This way, the resulting global position is unchanged, and the hexapod position has been moved to a feasible pose.

To compute this superimposed motion in the redundant DoF, an optimization algorithm is used that minimizes an objective function based on actuator extensions.

Research Questions

This paper explores an idea that integrates well with existing systems and promises to extend the workspace of a hexapod. However, some question are to be addressed:

1. How can redundant degrees of freedom be leveraged to extend the usable hexapod workspace?
2. How much workspace can be gained by exploiting redundant DoF?
3. What are the potential drawbacks and adverse effects of control strategies regarding redundant DoF?

Methodology

The algorithm presented in this paper computes a favorable position in terms of maximum working space in the redundant degrees of freedom of the simulator. This position is determined by an optimization algorithm based on an objective function applied to the extension of each actuator. Extensions that are close to the limits of the actuators' working space are penalized. The geometric relations of the Stewart platform (Stewart, 1965) lead to a formulation to compute the extensions of the individual actuators.

Inverse Hexapod Kinematics

A three-dimensional vector $r_{actuator,i}$, that describes the orientation and length of each actuator, is computed based on the actuator mounting positions of the moving base (mb) and static base (sb). The mounting points of the moving base are translated by rotation matrix C_{rot} and the translation vector r_{trans}.

$$r_{actuator,i} = C_{rot} r_{mb,i} + r_{trans} - r_{sb,i} \quad (1)$$

$$l_i = \|r_{actuator,i}\| - l_{center} \quad (2)$$

For the following optimization problem, the actuator state for each actuator is reduced to a one-dimensional variable l_i, which corresponds to the distance to the center zero position of the actuator.

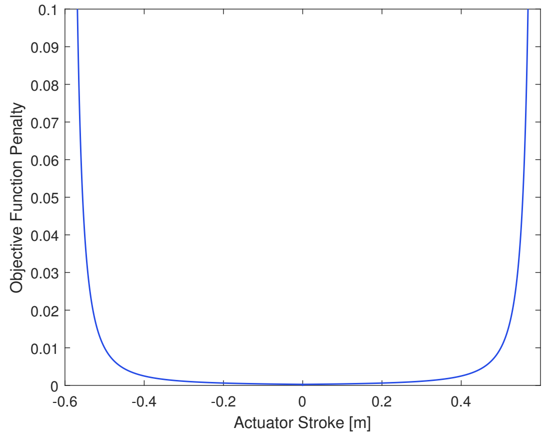

Figure 3: Objective function for an individual actuator

Objective Function

In order to maximize the workspace, it is assumed that the actuator stroke distance to the upper boundary (ub) and lower boundary (lb) must be maximized. To achieve this goal, an objective function is formulated, that is based on the inverse square law, as shown in Figure 3. Since the optimization algorithm may start at an infeasible pose, that contains invalid actuator positions, the inverse square law is only used up to a distance of ϵ to the actuator limits.

$$\epsilon > 0 \quad (3)$$

$$l_{ub,\epsilon} = l_{ub} - \epsilon \quad (4)$$

$$l_{lb,\epsilon} = l_{lb} + \epsilon \quad (5)$$

The objective function is continued beyond the shifted actuator boundaries as quadratic functions, that are C^2 continuous with respect to the inverse square function.

$$f_i = \begin{cases} 1 + k_1(l_i - l_{ub,\epsilon}) + k_2(l_i - l_{ub,\epsilon})^2 & \text{for } l_i > l_{ub,\epsilon} \\ \frac{\epsilon^2}{(l_{ub} - l_i)^2} & \text{for } l_i > 0 \wedge l_i < l_{ub,\epsilon} \\ \frac{\epsilon^2}{(l_{lb} - l_i)^2} & \text{for } l_i < 0 \wedge l_i > l_{lb,\epsilon} \\ 1 + k_1(l_{lb,\epsilon} - l_i) + k_2(l_{lb,\epsilon} - l_i)^2 & \text{for } l_i > l_{ub,\epsilon} \end{cases} \quad (6)$$

To combine the objective function of all actuators the infinity norm is used, as the hexapod workspace is restricted by the individual actuator, that is the closest to its limit.

$$f_{opt}(C_{rot}, r_{trans}) = \|f_1, .., f_6\|_\infty \quad (7)$$

Optimization Problem

The value of the objective function depends on the rotational and translational state of the simulator. The goal of the optimization problem is to minimize the objective function by manipulating the rotation or translation of the simulator along the redundant degrees of freedom. In this example, the translation r_{trans} in the y-direction is adjusted to a more favorable position with respect to the actuator extensions. The optimization problem is bounded by specifying upper and lower bounds for the optimization variable.

$$\min_{y \in \mathbb{R}} f_{opt}(C_{rot}, r_{trans} + y\ e_y) \quad (8)$$

$$\text{subject to } y < y_{ub} \wedge y > y_{lb} \quad (9)$$

Since the optimization problem has a fairly smooth and generally convex objective function, a gradient-based solver is used to find the minimum of the functional. In this work, the zero position was used as the initial value for the solver. For a motion cueing algorithm that makes use of this algorithm, it might be more appropriate to use the optimal value from the solution of the previous time step as the initial value.

Results

The results that are displayed in this section, are computed for the motion system of ika's highly dynamic driving simulator (Wagener, et al., 2023). This 7-DoF simulator features a Stewart platform, that is carried by a sled on a 12m long rail. The simulator is therefore redundant for translations in the y-direction.

First, the method is applied to an exemplary case, to show how the optimization scheme can be used to expand the workspace. The workspace is then systematically explored. In this way, it can be visually determined, where the highest workspace gains can be realized with the presented algorithm.

Exemplary demonstration case

Figure 1 shows a situation where a pose is requested from the Stewart platform that cannot be achieved without violating the stroke limits of the one actuator. The pose is a combination of a -0.26 rad yaw and a roll angle of 0.32 rad. High yaw angles combined with high roll angles can occur when the driving simulator renders the motion of a lane change during tilt coordination on a curved road. To isolate the effect in the yaw-roll plane, all other variables are set to zero.

In Figure 4, the objective function is plotted against the y-position of the hexapod. The objective function decreases toward the green region, which indicates feasible hexapod positions. An optimization solver converges to an optimal y-position of -0.22 with respect to the objective function. If the hexapod is moved to the left relative to the sled and the sled is simultaneously moved to the right by the same distance, the actuator limit violation can be resolved. Figure 2 shows the optimal pose and illustrates that the previously unattainable position can be achieved by freezing the global simulator position and adjusting the sled position.

Workspace Envelope Evaluation

By performing a grid search in Cartesian space and checking in actuator space, if the requested poses are valid, the workspace envelope can be computed. A grid is spanned in the dimensions of the simulator and for each grid point it is determined, whether the pose can be reached starting from the current operating point. By analyzing the available workspace, the potential of the algorithm to extend

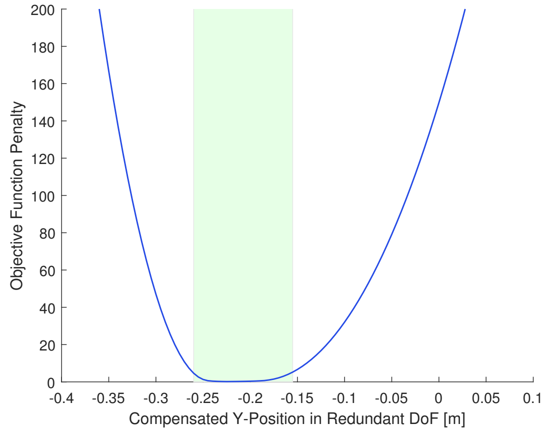

Figure 4: Objective function over redundant DoF (roll=0.26 rad, pitch=0 rad, yaw=0.32 rad, x=0, y=0, z=0, rail=0)

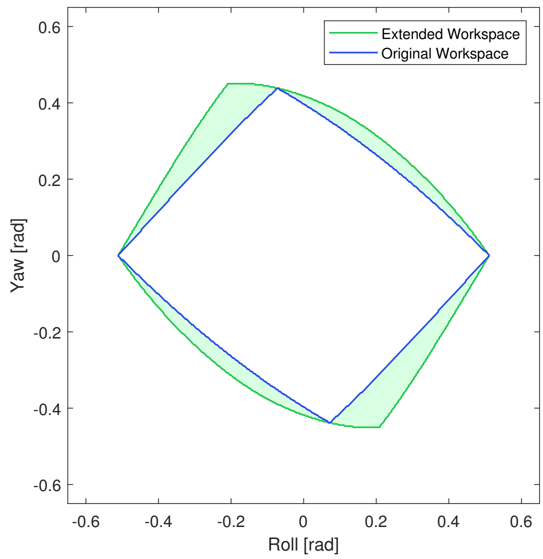

Figure 5: Roll-Yaw Workspace (pitch=0,x=0,y=0,z=0,rail=0)

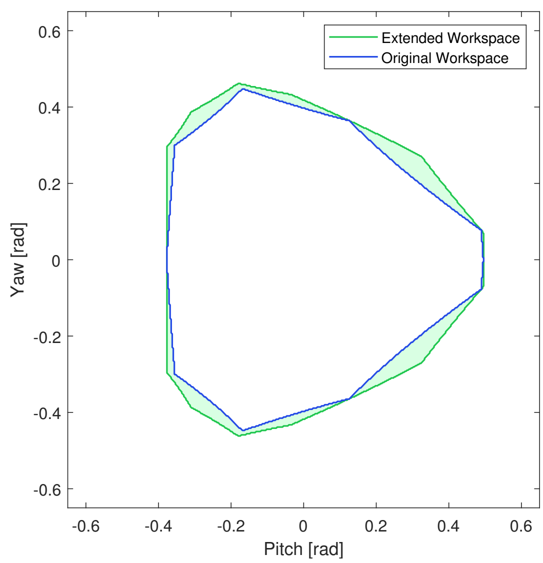

Figure 6: Pitch-Yaw Workspace (roll=0,x=0,y=0,z=0,rail=0)

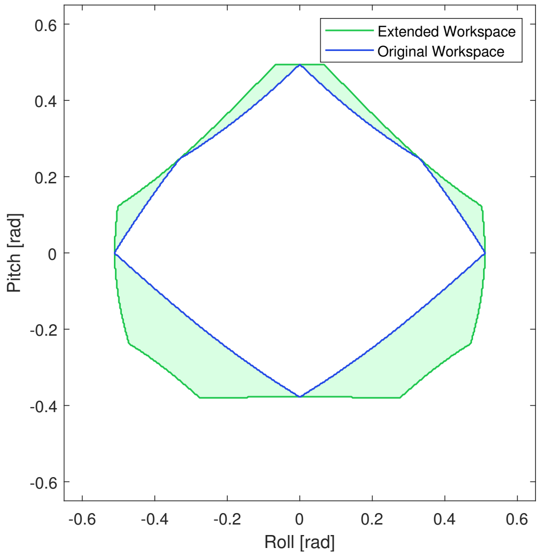

Figure 7: Roll-Pitch Workspace (yaw=0,x=0,y=0,z=0,rail=0)

the workspace into non-redundant degrees of freedom depending on the situation is evaluated. Special attention is given to chained rotations and rotational limits.

In Figure 5, the area enclosed by the blue line represents the workspace of a Stewart platform in the roll-yaw plane. Since all other DoFs are set to zero, the maximum achievable yaw angle as a function of roll angle is represented by the blue outline. Adding the optimal translation in the redundant DoF to the equation increases the available workspace. The green area shows poses that can be achieved by superimposing the hexapod motion in the redundant degree of freedom. The maximum yaw angle at zero roll angle cannot be improved. The workspace expansion algorithm shows the most gains when multiple degrees of freedom are used simultaneously. The total area gained in the roll-yaw plane is 16.2 %.

The workspace between yaw and pitch angles, Figure 6, is asymmetric in the pitch direction. This means that the simulator can pitch further forward than backward. The workspace gains in this slice are rather small, a 7.6 % surface area gain, as the actuators are already used efficiently in the investigated layout of hexapod and rail. Most of the workspace gains can be realized in the roll-pitch plane, see figure 7. The workspace grew by 24.6 % in comparison to the base workspace. Especially for negative pitch angles, there is much more space for the simulator to roll, when using the compensatory motion algorithm.

Conclusion

By effectively extending the hexapod workspace, the presented method allows to improve the performance of existing motion cueing algorithms, in particular for maneuvers that demand motion in multiple degrees of freedom simultaneously. In the roll-pitch plane, relevant for braking maneuvers under lateral tilt coordination, workspace gains of over 20 % can be realized. This allows for a more aggressive parameterization of motion cueing algorithms. Motion algorithms that do not account for the interdependence of degrees of freedom can use the motion system more efficiently by integrating this method.

For motion cueing algorithms that already incorporate dependent motion constraints of the motion platform, the method could be used to control one redundant degree of freedom. This would allow the motion cueing algorithm to solve for one less degree of freedom and thus reduce its computation time.

Future work

The slices through the rotating workspace give a good idea of workspace gains that can be achieved. A three-dimensional workspace analysis could provide more comprehensive insights (Masory and Wang, 1994). The concept of running an optimization scheme to find a suitable position in redundant DoFs can also be applied to rotational DoFs, such as yaw tables, to open up new motion spaces.
The next step is to roll out this method to a real driving simulator to verify its robustness and dynamic performance under real-world conditions. As compensating motions are applied to a coupled motion system this method is very sensitive to system latencies. The effects of real world latencies and system control responses will be investigated.

Acknowledgements

The work of this paper has been done in the context of the SUNRISE project which is co-funded by the European Commission's Horizon Europe Research and Innovation Programme under grant agreement number 101069573. Views and opinions expressed, are those of the author(s) only and do not necessarily reflect those of the European Union or the European Climate, Infrastructure and Environment Executive Agency (CINEA). Neither the European Union nor the granting authority can be held responsible for them

References

Baumann, G., Riemer, T., Liedecke, C., Rumbolz, P., and Schmidt, A., 2012. How to build Europe's largest eight-axes motion. In: Driving Simulation Association ed. *DSC 2012 Proceedings*. FRANCE.

Ellensohn, F., Spannagl, M., Agabekov, S., Venrooij, J., Schwienbacher, M., and Rixen, D., 2020. A hybrid motion cueing algorithm. *Control Engineering Practice*, 97. ISSN: 0967-0661. https://doi.org/10.1016/j.conengprac.2020.104342.

Fang, Z., Wautier, D., and Kemeny, A., 2021. Renault's new MPC based motion cueing algorithm development. In: Driving Simulation Association ed. *DSC 2021 Proceedings*. FRANCE.

Masory, O. and Wang, J., 1994. Workspace evaluation of Stewart platforms. *Advanced Robotics*, 9(4), pp. 443–461. ISSN: 0169-1864. https://doi.org/10.1163/156855395X00508.

Stewart, D., 1965. A Platform with Six Degrees of Freedom. *Proceedings of the Institution of Mechanical Engineers*, 180(1), pp. 371–386. ISSN: 0020-3483.

Wagener, N., Russ, F., Beckmann, J., Legran, P., and Eckstein, L., 2023. ika's highly dynamic driving simulator. In: Driving Simulation Association ed. *DSC 2023 Proceedings*. FRANCE.

Zeeb, E., 2010. Daimler's New Full-Scale, High-dynamic Driving Simulator – A Technical Overview. In: Driving Simulation Association ed. *DSC 2010 Proceedings*. FRANCE.